



	<b>Experiment title:</b> Structure formation in artificial extracellular matrix materials under strain	<b>Experiment number:</b> 26-02-685
<b>Beamline:</b> BM26B	<b>Date of experiment:</b> from: 21/7/2014 to: 25/7/2014	<b>Date of report:</b> 26/9/2014
<b>Shifts:</b> 9	<b>Local contact(s):</b> Dr. Giuseppe Portale	<i>Received at ESRF:</i>
<b>Names and affiliations of applicants (* indicates experimentalists):</b>  Dr. Paul H.J. Kouwer* Radboud University Nijmegen Institute for Molecules and Materials Heyendaalseweg 135 6525 AJ Nijmegen The Netherlands		

## Report:

### Goals

The final goal of the experiment was to investigate the impact of strain on the structure of a strain-stiffening synthetic hydrogel. To achieve our goals, we need to first look at the scattering patterns of the gels at zero shear. To obtain sufficient information on the scattering characteristics, we investigated the gel at different conditions: (a) at different concentrations; (b) gels of different polymer lengths; and (c) gels in different salt solutions.

### Motivation

Hydrogels are currently investigated for their biomedical applications, in particular in drug delivery, wound healing and tissue engineering. Although many synthetic polymers for tissue engineering have been suggested and developed, physicians most often employ biopolymers, despite all intrinsic disadvantages, research points out that these materials outperform the synthetic ones. A major difference between synthetic and biological gels is their mechanical response to deformation. Whereas in synthetic gel, the stiffness is a constant, in biogels it is a function of applied stress; on increasing strain, the modulus can easily increase a factor 100 or even more. Recently, we reported a synthetic hydrogel that shows the same strain-stiffening behaviour, and more importantly, also in the same strain and stress regime.<sup>1,2</sup> Also its morphology is similar to that of the biogels. This morphology, the bundled structure, however, is extremely difficult to probe reliably in situ. With SAXS, we would like to study the structure of these hydrogels. Scattering data on strained samples, both in the linear and the stiffening regime can provide valuable information on the fundamental mechanisms of strain-stiffening, which has implications for the design of other artificial strain-stiffening materials, as well as for the applications of these materials in biomedical field.

## Setup

Scattering patterns were collected on beam line BM26B with a 2D Pilatus1M detector placed at 3.5m from the sample. In the first part of our experiment we study the scattering patterns of the gel in capillaries. Temperature control between 5 and 50 °C gives the opportunity to follow the transition from a (low viscous) polymer solution (at low temperature) to an elastic gel (at elevated temperature). In the final stage of the experimental time, we performed measurements under stress using a Linkam strain device. Although a strain can be applied in the device, no mechanical feedback (like in a rheometer) is obtained.

## Results and discussion

Part A: capillary measurements. In the capillary setup, we measured scattering profiles as a function of: (i) temperature, (ii) polymer concentration and (iii) polymer length.

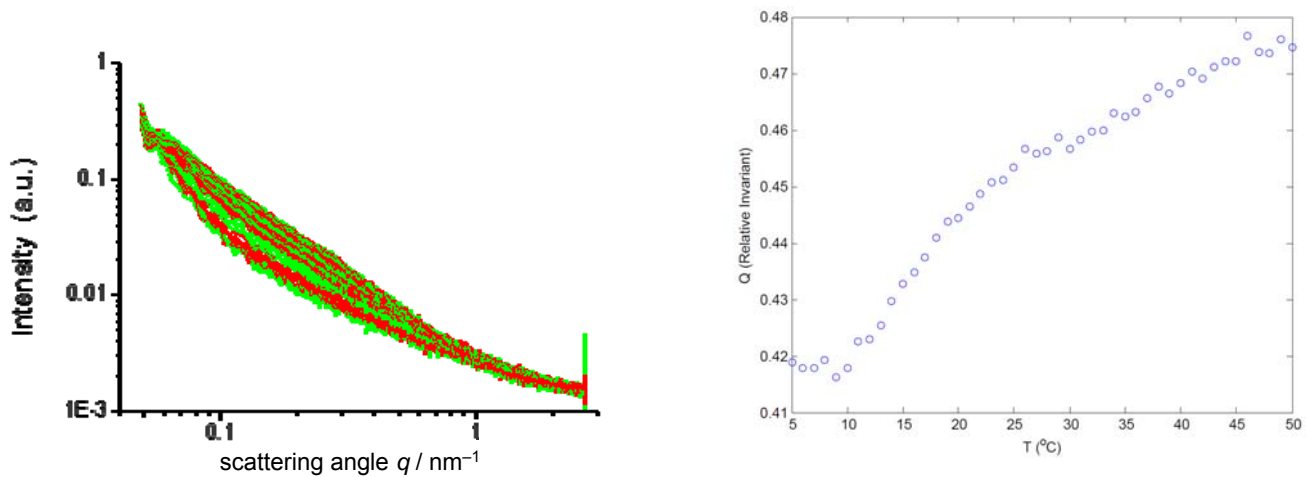


**Figure 1.** Scattering profiles (left) and corresponding invariant of **P2000f** (default polymer length  $M_v = 400 \text{ kg/mol}$ ) at default concentration  $c = 5 \text{ mg/mL}$  as a function of temperature (exposure time: 10 s). At temperatures below gelation temperature  $T_{\text{gel}} = 19 \text{ °C}$ , the sample is a low-viscous polymer solution; above  $T_{\text{gel}}$ , the sample is an elastic hydrogel.

The scattering profiles at larger angles are independent of temperature (Fig. 1, left), but show a small dependence at smaller angles as a result of hydrogel formation. The invariant as a function of temperature (Fig. 1, right) shows clearly that gelation sets in above 10 °C. The transition temperature is in line with DSC experiments, where the onset of the phase transition also is below  $T_{\text{gel}}$ . The increase in scattering intensity at  $q = 0.1\text{--}0.2 \text{ nm}^{-1}$  is attributed to the bundling process in the hydrogel. The invariant (Fig. 1, right) also shows a second regime at  $T > 25 \text{ °C}$  where its slope changes.

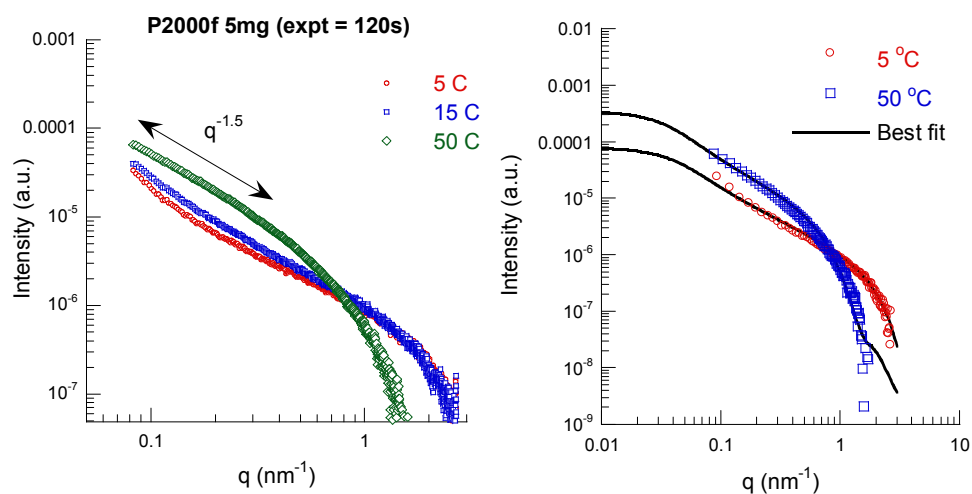


**Figure 2.** Scattering profiles (left) and fits (right) of **P2000f** ( $c = 5 \text{ mg/mL}$ , exposure time 120 s) at various temperatures in solution (5, 15 °C) and in the hydrogel (50 °C). The scattering profiles were fit to a simple cylinder model.

The featureless scattering curves were fit to a straightforward cylinder model (Fig. 2) to retrieve structural network parameters. In the gel phase at 50 °C, we fit an average bundle persistence length  $l_p = 18$  nm and a characteristic bundle length of  $\sim 200$  nm. Both numbers are in line with what would be expected for the PIC hydrogels, based on macroscopic rheology experiments.<sup>1</sup> In addition, these numbers compare well to structurally similar methylcellulose hydrogels.<sup>3,4</sup> At lower temperature, in the solution phase, we find molecular lengths of  $\sim 250$  nm, which is a very good match to the results obtained by viscometry experiments.<sup>5</sup>

Samples at different concentrations (range 1–5 mg/mL) show very similar scattering profiles, in particular at the  $q = 0.1$ – $0.2$  nm<sup>-1</sup> range, where the bundles scatter (Fig. 3). The current thought that the network morphology (i.e. the bundle size) is independent from concentration is based on AFM studies of dried hydrogels, which means that they are not very reliable. The scattering results from the concentration series is much better experimental evidence to support the controlled bundle size concept.

Finally, we studied the scattering intensity as a function of the polymer length, as determined by viscometry measurements. Figure 4 shows the scattering intensities at  $q = 0.2$  nm<sup>-1</sup> (where the bundles scatter) corrected for the background scattering of the individual polymer chains recorded at  $T = 5$  °C. The figures show that below  $T = 30$  °C, the curves are more or less identical (since no chains are formed yet at low  $T$ ), and that at elevated temperatures, the curves deviate. The strongest increase in intensity is formed by the shortest polymers, possibly due to a stronger aggregation behaviour of the shortest polymers with a molecular length significantly shorter than the molecular persistence length  $l_{p,0}$ .<sup>6</sup>

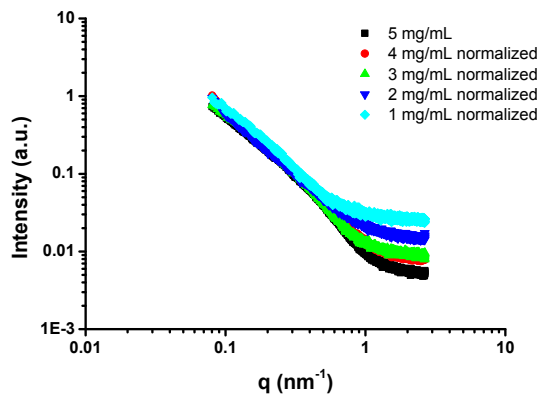


**Figure 3.** Scattering profiles of **P2000f** at  $T = 50$  °C in a  $c = 1$ – $5$  mg/mL concentration range, normalised for concentration. The curves perfectly overlap in the  $q = 0.1$ – $0.4$  regime, indicating highly comparable network geometries.

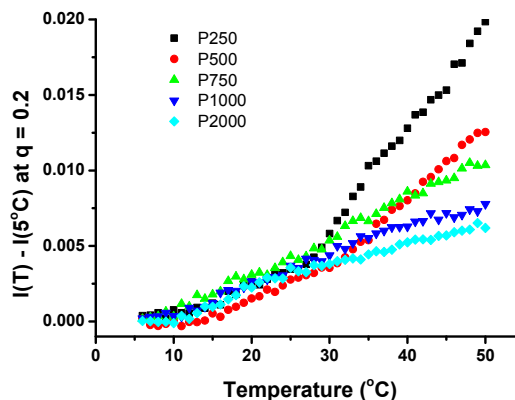


**Figure 4.** Scattering intensities at  $q = 0.2$  nm<sup>-1</sup> of different molecular weight polymers ( $M_v = 140$  kg/mol for **P250** to  $M_v = 400$  kg/mol for **P2000f**) at  $T = 50$  and  $c = 1$ – $5$  mg/mL. The solution spectra (recorded at  $T = 5$  °C) were first subtracted.

Part B: strain cell measurements. To probe the scattering in the nonlinear mechanical regime of these polymers, we inserted a sample in a Linkam strain cell, which we mounted in the beam. The strain cell is designed to apply controlled deformations to a sample, but has two major limitation for our intended use: (i) the cell provides no mechanical feedback of the sample. It will not be noticed when at elevated strains a sample (temporarily) detaches from the cell. This will relieve stress from the sample and renders the ultimate measurement (scattering as a function of stress) highly unreliable. In addition, the cell requires thick samples, which increases the changes of detaching (in particularly with the large negative normal stresses that are commonly observed for strain stiffening materials)<sup>7</sup> and, additionally, consumes copious amounts of sample. Both challenges are addressed by a rheometer, which is currently redesigned to fit on the DUBBLE beam line.

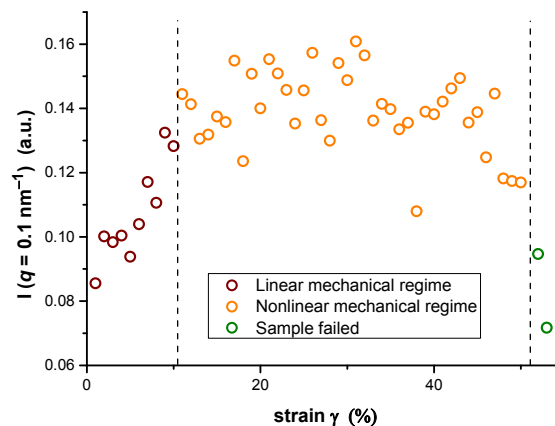


**Figure 5.** Scattering intensities at  $q = 0.1$  nm<sup>-1</sup> (**P2000f**,  $T = 37$  °C,  $c = 5$  mg/mL) as a function of applied strain  $\gamma$  in the strain cell.

The preliminary results obtained by the stress cell (Fig. 5) show that at small angles (where the bundles are probed) the scattering intensity is a function of the applied strain. In the low-strain regime, the scattering intensity quickly increases with  $\gamma$ . The primary network response in this regime is bending of the bundle structure. At increased strains, a network of semi-flexible polymers (like the PIC hydrogels) becomes strain stiffening. Rheology experiments show that the critical strain, the strain where the mechanical response changes from linear to nonlinear, is  $\sim 10\%$ .<sup>5</sup> The network responses changes to a stretch-dominated mechanism. Exactly at these strains, the scattering profile becomes strain-independent (although substantial noise is present in the measurement). At high strains (here at  $\gamma > 50\%$ ), the sample fails and the scattering signal drops quickly.

Although the preliminary measurement looks encouraging, the lack of mechanical feedback is a main concern. Is the sample truly 50 % strained by the end of the measurement? Or did it occasionally detach from the plate and is the true strain only 15 %. A rheometer that provides mechanical feedback is desirable to do this type of experiments.

## Conclusions

In conclusion, SAXS is an excellent tool to gain more insight in the structural changes that take place during hydrogel formation. SAXS experiments, for instance, clearly demonstrate that the network structure is not dependent of concentration, something that was so far only assumed based on AFM experiments.

Furthermore, the changing network morphology as a function of strain can be studied using SAXS in combination with a strain cell, but is much more convenient when SAXS is combined with a rheometer as this provides direct mechanical feedback of the sample. A combined rheoSAXS setup with a dedicated shear geometry will be used in the near future.

- 1 Kouwer, P. H. J. *et al.* Responsive biomimetic networks from polyisocyanopeptide hydrogels. *Nature* **493**, 651-655 (2013).
- 2 Koepf, M. *et al.* Preparation and characterization of non-linear poly(ethylene glycol) analogs from oligo(ethylene glycol) functionalized polyisocyanopeptides. *Eur. Polym. J.* **49**, 1510-1522 (2013).
- 3 Lott, J. R. *et al.* Fibrillar Structure in Aqueous Methylcellulose Solutions and Gels. *Macromolecules* **46**, 9760-9771 (2013).
- 4 Lott, J. R., McAllister, J. W., Arvidson, S. A., Bates, F. S. & Lodge, T. P. Fibrillar structure of methylcellulose hydrogels. *Biomacromolecules* **14**, 2484-2488 (2013).
- 5 Jaspers, M. *et al.* Ultra-responsive soft matter from strain-stiffening hydrogels. *Nat. Commun.* **5**, 5808 (2014).
- 6 Pandolfi, R. J., Edwards, L., Johnston, D., Becich, P. & Hirst, L. S. Designing highly tunable semiflexible filament networks. *Phys. Rev. E* **89**, 062602 (2014).
- 7 Janmey, P. A. *et al.* Negative normal stress in semiflexible biopolymer gels. *Nat. Mater.* **6**, 48-51 (2007).